IEEE Access
Multidisciplinary | Rapid Review | Open Access Journal

Date of publication xxxx 00, 0000, date of current version xxxx 00, 0000.

Digital Object Identifier 10.1109/ACCESS.2017.Doi Number

Automatic Voltage Stabilization Using IGBT Based on Load Tap Changer with Fault Consideration

Ali Ahmed Adam Ismail[1], Humaid Alsuwaidi[1,2], and A. Elnady[1,3]

[1]Electrical Engineering Department, University of Sharjah, P. O. Box: 27272 Sharjah, UAE
[2]DEWA, Dubai Electricity and Water Authority, P.O. Box 564 - Dubai - UAE
[3]Electrical and Computer Engineering Department (Adjunct), Royal Military College, Kingston, Ontario, Canada

Corresponding author: Ali Ahmed Adam Ismail (e-mail: aliadam999@yahoo.com).

"This work was supported in part by the University of Sharjah. Department of Electrical Engineering."

ABSTRACT In this work, a voltage regulation scheme to stabilize voltage variation in the consumer side is proposed. The voltage regulation scheme uses IGBT-based onload tap changer (OLTC) and nonlinear hysteresis control algorithm. The proposed switching algorithm establishes the commutation of the taps without redundant short circuit operation of the taps. The experimental results of the designed system show accurate voltage regulation at the consumer side and high ability of the designed system to fix voltage sag and voltage swell in maximum of one cycle period. The paper considers the consequences of fault in the drive circuit of the IGBT tap changer and discusses its reliability. The analysis and the experimental results of the faults in the drive circuit show that the loss of one drive signal results in a large circulating DC current in the primary circuit and may result in fault current of value more than three times the operated current, which leads to unavailability of the system.

INDEX TERMS On load tap changer, voltage regulation, distribution transformer, IGBT, OLTC fault analysis.

I. INTRODUCTION

Voltage/power quality in the power system requires stable voltage with certain variation limit to be delivered to the consumers irrespective of the variation in the generation, transmission or in the distribution system. However, due to increased renewable energy resources connected to the grid, and demand change, the voltage in the distribution system is not always constant. This unwanted variation in the voltage requires an adoption of adequate and fast response regulation system. This voltage regulation system ensures an acceptable voltage level of electricity to the consumers. In the distribution system, the voltage regulation is considered as one of the most important and significant power quality problems [1]-[5].

Load tap changers (or voltage regulation transformers) have been used widely in the distribution systems to regulate the voltage magnitudes over feeders. The tap position of these transformers is traditionally controlled by means of the local voltage measurements [6]. This method is considered not suitable [7] in presence of the bidirectional power flows especially when optimality of the power flow is not considered. Thus, it has been studied numerically with help of optimal control algorithm to automatically regulate the feeder voltages with the minimum errors [8, 9]; but there is no experimental data available to support the effectiveness of the methods in [8, 9]. Nowadays, both electromechanical and electronics on-load tap changers (OLTCs) are used to automatically stabilize the voltage in the consumer side.

Electromechanical OLTCs have been used in the medium- and high-power systems to handle the line tap commutation and regulate the voltage automatically. The commutation of the taps in these electromechanical devices invokes arcing, which carbonizes the contacts and results in continuous maintenance requirements in such a way that degrades its operation [10]-[13]. Electronic switches have started to replace the mechanical switches in the OLTC with no arcing and with a capability to withstand high voltage and current. The electronic switches used in OLTC include Thyristors, Triacs and IGBTs.

Thyristors have the advantage of its capability to handle high current and high voltage as compared to other electronic switches. These Thyristors have been used to replace the mechanical switches that are used in the high voltage networks [14]-[18]. Thyristors successfully overcome the traditional arcing problems and result in a free of arc switching commutation. The main disadvantage of these switches is the holding current that keeps two

This article has been accepted for publication in a future issue of this journal, but has not been fully edited. Content may change prior to final publication. Citation information: DOI 10.1109/ACCESS.2021.3079507, IEEE Access

thyristors in operation at the same instant, which results in inter-tap short circuit [14, 15, 18]. Although many modifications with current limiters [16] or with auxiliary transformers [17] have been employed to resolve this issue, thyristors are still suffering of many unresolved problems such as slow switching operation, and the complexity of the control circuit. The Traic based OLTC as well has been used [19], but it is suffering of the same drawbacks of the thyristors.

Recently, the IGBT based OLTC has been used successfully to replace the thyristor based one [20]-[22]. However, the power handling capability of IGBT is limited; it has the advantage of high-speed operation and less gate drive requirements. In most of the proposed IGBT based OLTC [20]-[22], the authors have adopted overlap of tap operation like that used with thyristors [14]-[18] during commutation, which degrades the full functionality of the OLTC transformer. The fast operation of IGBT permits the usage of dead time during the taps commutation to provide enough secure separation of the tap without disturbing the continuation of the power to the consumers.

Although the electronics OLTCs provide fast and free of arc taps commutation, faults in the drive circuits of these switches may deteriorate its functionality and result in low reliable system. The consequences of fault in drive circuit or in power electronics have been handled in the literature [23]-[27] for machines drive circuits, however, it has not been yet applied to electronics OLTC.

The main contributions of this paper include novel simple analysis of the OLTC during normal and faulty operation, fast response OLTC design with detailed nonlinear control algorithm, new result performance for fault in drive circuit as well as new result for fast sag and swell voltage compensation.

This paper is organized as follows: Section II gives the proposed topology outline and the algorithm of the nonlinear control loop. Section III explains the analysis of the proposed system including normal operation and drive fault analysis. Section IV presents the experimental validation results, including normal voltage regulation, compensation of voltage sag and swell, as well as fault results.

II. THE PROPOSED TOPOLOGY

Fig.1 shows the proposed system topology. The designed system in Fig. 1 composes of power electronics switching arrangement, drive circuit block, voltage and current sensor systems, and nonlinear control algorithm block. The power electronics switching elements utilize bidirectional IGBT switches arrangement connected in common emitter mode [22, 28] to decrease the overall drive circuit requirements. Each bidirectional switch in the arrangement has common ground and common gate signal. This arrangement enables us to control the switching in one-step time, which reduces the level of the drive failure and increases its reliability. We have connected the switches in series with fast melting fuses

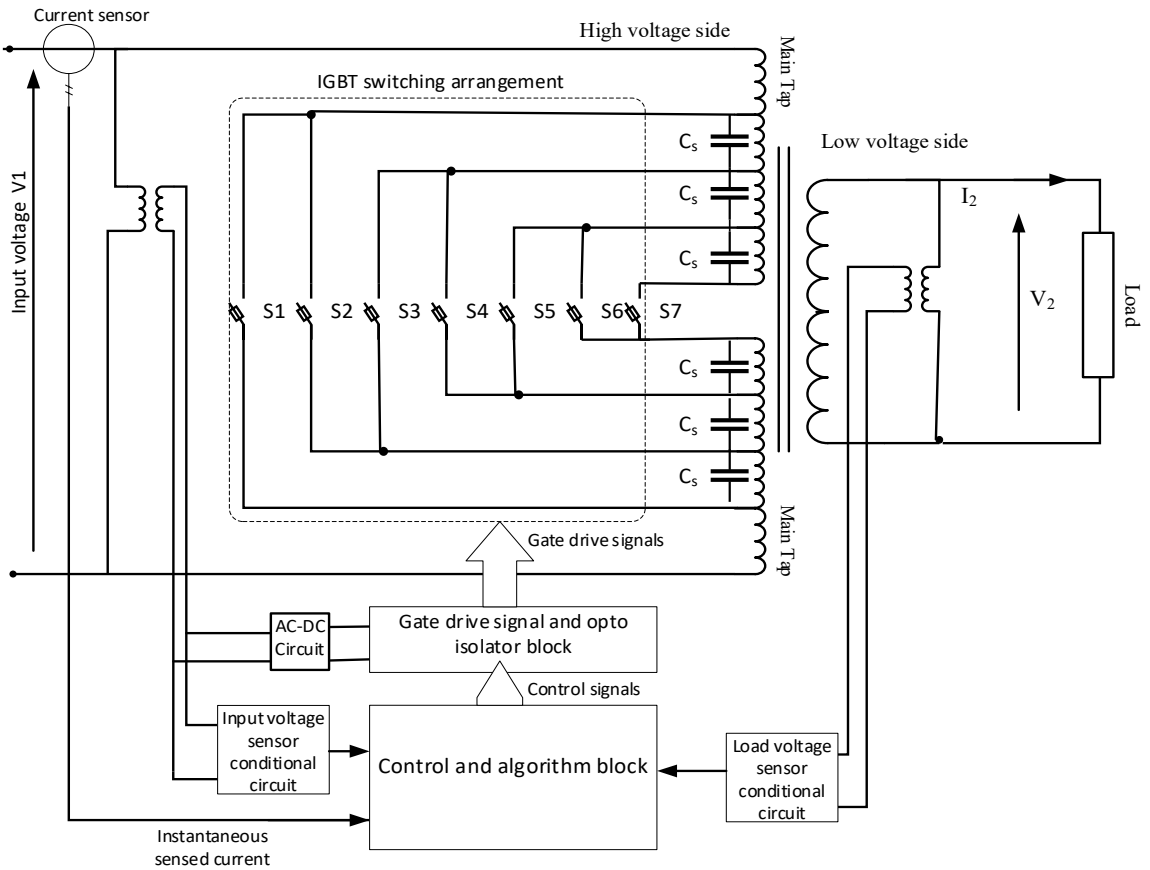

FIGURE 1. The proposed IGBT based on load tap changing transformer topology.

This article has been accepted for publication in a future issue of this journal, but has not been fully edited. Content may change prior to final publication. Citation information: DOI 10.1109/ACCESS.2021.3079507, IEEE Access

to provide protection during inter-taps short circuit. To decrease voltage surges during tap commutation, the algorithm utilizes the instantaneous sensed input current to carry out the switching during zero crossing instants. Additionally, snubber capacitors have been used across the tap to ensure minimum voltage surges during tap commutation. To achieve the overall required voltage control operation, the control algorithm utilizes an input voltage sensor, output voltage sensor and an input current sensor. The designed algorithm achieves smooth transition of the taps without contact sparking and without interrupting the flow of the power to consumers. The control algorithm achieves the smooth transition of the taps directly (without taps overlapping as the case in [13, 22]) by inserting 2 μs dead time during tap commutation. The designed algorithm as well, can handle the normal voltage regulation and can amend the abnormal grid transient problems such as voltage sag and voltage swell. The following section describes this control algorithm.

A. THE SUGGESTED CONTROL ALGORITHM

Fig. 2 shows the suggested control block diagram. The input to the block is the measured primary rms voltage, the measured secondary rms voltage, the measured primary instantaneous current, and the input reference voltage (the desired load voltage) in the secondary side. The control algorithm works within certain input voltage range, for extreme high input voltage or extreme low input voltage (LV), the control algorithm switches off the transformer and no power transfers to the load. For input voltage within the controller range, the control algorithm compares the secondary voltage ($V_{2\text{-}rms}$) with the reference voltage (V_{ref}) and generates an error signal given as,

$$\Delta v = V_{ref} - V_{2-rms} \tag{1}$$

The error signal passes through nonlinear controller block, which is composed of the multilevel hysteresis controller, and an inner limiter control loop. The output of the multilevel hysteresis controller in Fig. 3 is an offset integer "τ"; where $\tau \varepsilon \{-3, -2, -1, 0, 1, 2, 3\}$. The algorithm of the hysteresis controller follows the logic in (2) corresponding to the setting of the hysteresis bandwidth "h". The control algorithm adds the offset "τ" to the previous tap number and passes the resultant through tap limiter to generate the new tap switching number. The control algorithm works on the selected new tap number to provide the adequate triggering signals to the IGBTs to set the desired reference voltage. This algorithm forces the switching of the IGBTs to take place at zero-crossing points of the transformer primary current.

Fig. 4 shows the tap switching transition state diagram corresponding to the calculated offset value. We have designed the commutation of the taps in such a way to permit a direct transition of the taps up to three level tap-voltages without passing through the center tap (tap4), this direct transition of the taps enables the designed OLTC to withstand sag and swell problems in the shortest possible time.

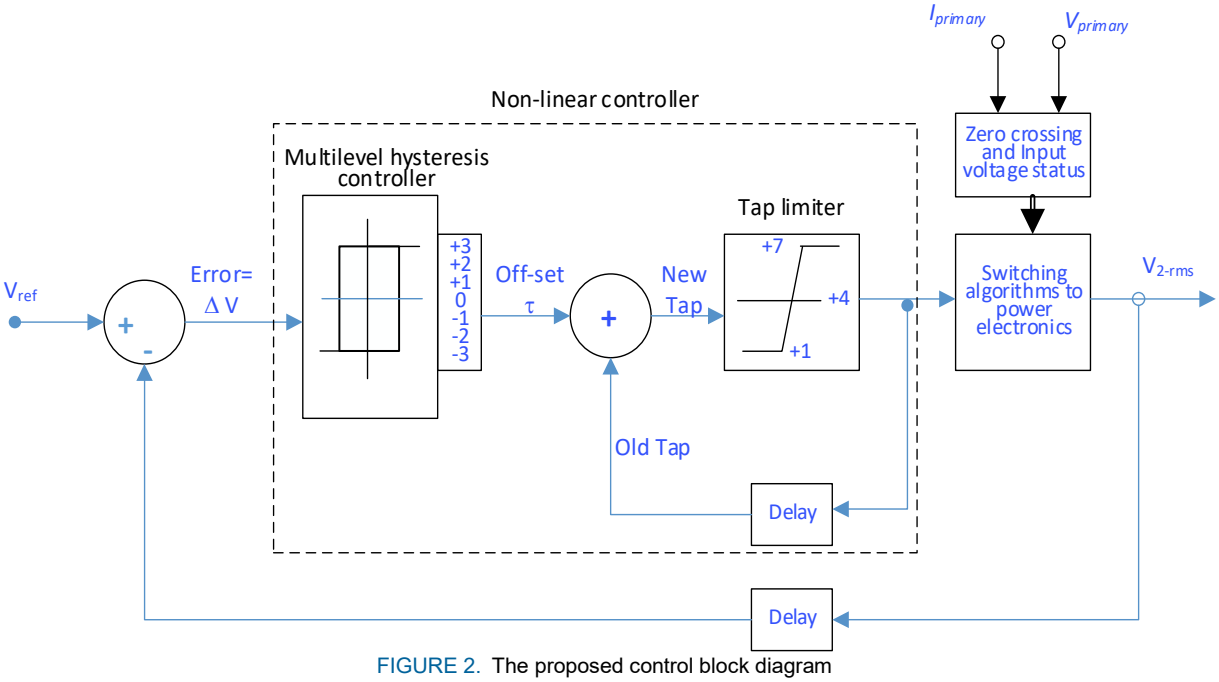

FIGURE 2. The proposed control block diagram

This article has been accepted for publication in a future issue of this journal, but has not been fully edited. Content may change prior to final publication. Citation information: DOI 10.1109/ACCESS.2021.3079507, IEEE Access

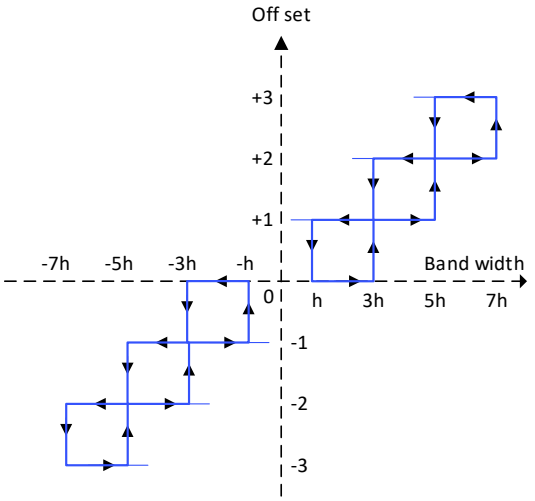

FIGURE 3. Multilevel hysteresis controller with error bandwidth equal to "2h".

$$\tau = \begin{cases} +3 \quad if \quad (5h < \Delta v \le 7h) \\ +2 \quad if \quad (3h < \Delta v \le 5h) \\ +1 \quad if \quad (h < \Delta v \le 3h) \\ 0 \quad if \quad (-h < \Delta v \le +h) \\ -1 \quad if \quad (-3h < \Delta v \le -h) \\ -2 \quad if \quad (-5h < \Delta v \le -3h) \\ -3 \quad if \quad (-7h < \Delta v \le -5h) \\ else\ Tap = 4;\ \tau = 0; \quad \text{activate center tap} \end{cases} \tag{2}$$

III. ANALYSIS OF THE PROPOSED SYSTEM

In this section, we have performed the electrical analysis of the proposed switching system and the relationships of the currents and voltages in both the transformer primary and secondary side. The analysis includes both the normal operation of the transformer when the complete system is available as well as the case when the system under fault conditions.

A. NORMAL OPERATION

Fig. 5 shows the redrawing of the electric circuit of the seven-tap changing transformer system without the control circuit and the snubber capacitors to simplify the analysis. In Fig. 5-a, the switches S_1 to S_7 are bidirectional switching combination. Each switch composes of two IGBTs with antiparallel diodes, the IGBTs have a common emitter arrangement as shown in Fig. 5-b. Fig. 6 gives the transformer operational equivalent circuit of Fig. 5-a referred to the transformer primary side.

where:

"k" represents the tap number (switch number) connected to the main winding,

R_p, jX_p represent the leakage resistance and inductance of the main winding,

R_{tap}, jX_{tap} represent the leakage resistance and inductance of one tap winding.

R_m, jX_m represent the equivalent resistance of the core loss and the inductance of the magnetization circuit, respectively.

The transformer primary leakage impedance during the closing of switch "k" is:

$$R_1 + jX_1 = (R_p + (k-1)R_{tap}) + j(X_p + (k-1)X_{tap}) \tag{3}$$

where, *(k-1)* gives the number of taps connected in series with the main winding.

The secondary referred impedance in (4) is composed of the load-referred impedance (R'$_L$ + jX'$_L$) in series with the transformer secondary referred leakage impedance (R'$_s$+jX'$_s$),

$$R_2' + jX_2' = (R_s' + R_L') + (jX_s' + jX_L') \tag{4}$$

Using nodal analysis, (5) expresses the voltage of node "E" (Fig. 6) under normal operating condition,

$$E = \frac{V_1}{R_1 + jX_1} * \left(\frac{1}{\frac{1}{R_m} + \frac{1}{jX_m} + \frac{1}{R_1 + jX_1} + \frac{1}{R_2' + jX_2'}} \right) \tag{5}$$

Through the formula given in (5), it is possible to express the secondary voltage at the load terminals as:

$$V_2 = \frac{N_2}{N_{11} + (k-1)N_{tap}} * \frac{V_1}{R_1 + jX_1} * \frac{R_L' + jX_L'}{R_2' + jX_2'} * \left(\frac{1}{\frac{1}{R_m} + \frac{1}{jX_m} + \frac{1}{R_1 + jX_1} + \frac{1}{R_2' + jX_2'}} \right) \tag{6}$$

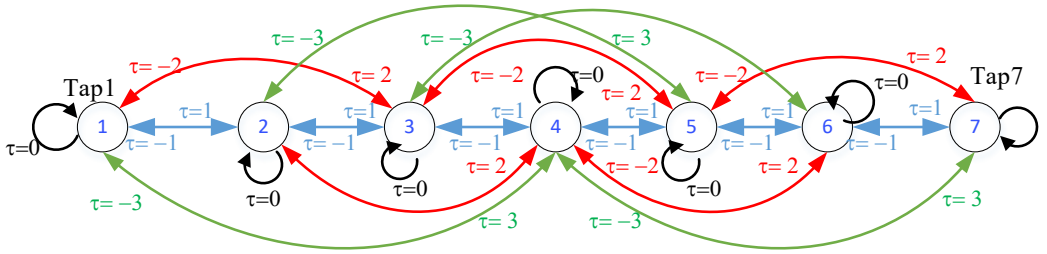

FIGURE 4. Suggested tap state transition diagram corresponding to the generated offset value τ

This article has been accepted for publication in a future issue of this journal, but has not been fully edited. Content may change prior to final publication. Citation information: DOI 10.1109/ACCESS.2021.3079507, IEEE Access

where:
N_2: the number of turns in the secondary side.
N_{11}: the number of turns in the main primary winding.
N_{tap}: the number of turns per tap in the primary side.

Using (5) and (6) we can express the primary current and the secondary current as in (7) and (8) respectively,

$$I_1 = \frac{V_1 - E}{R_p + (k-1)R_{tap} + j(X_p + (k-1)X_{tap})} \quad (7)$$

$$I_2 = \frac{E}{R_2' + jX_2'} * \left(\frac{N_{11} + (k-1)N_{tap}}{N_2}\right) \quad (8)$$

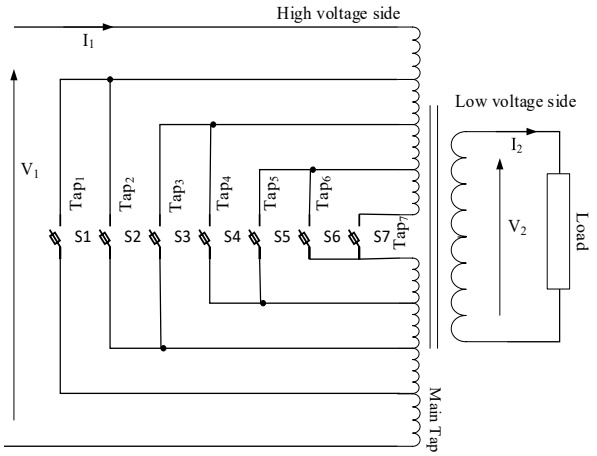

(a)

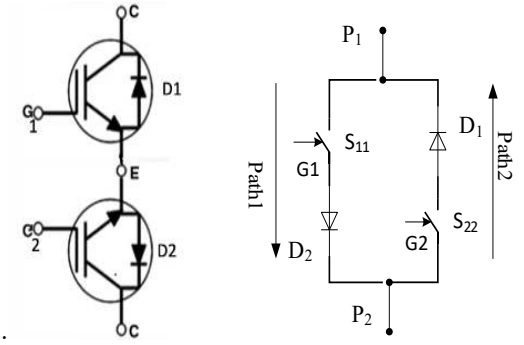

(b)

FIGURE 5. Electric circuit digram of the seven tap changing transformer: (a) Circuit outline (b) IGBT bidirectional switch and equivalent current paths circuits

B. RELIABILITY ASPECT AND DRIVE FAULT ANALYSIS

Besides the accurate performance, the proposed system should function safely with high availability and reliability. The proposed electronic tap change module composes mainly of bidirectional IGBT switches, diodes, sensors, and control algorithm system (Microcontroller + software). Failure in one of these items may result in partial or complete unavailability of power transfer to the load. In drive system utilizing IGBT switches, the authors in [23]-[26] have reported that around 38% of the faults are due to power devices. In addition, many publications have emphasized on the IGBT gate drive open circuit faults and IGBT short circuit faults [24]-[27], because these faults lead to catastrophic failure of the whole system. The short analysis of the fault in this section gives the most severe power electronics faults and their impact on the OLTC reliability.

Considering the bidirectional switch of the IGBT and its ideal equivalent operational circuit as given in Fig. 5-b. All the switches S_{11}, S_{22}, D_1, and D_2 must work properly during a complete cycle period to pass safely the AC power between point P_1 and point P_2. A fault in one (or combination) of these components or in the drive signals G_1 and/or G_2 result in a significant degraded performance or complete mal function of the system. The possible resulted failures include complete open circuit between points P_1 and P_2, permanent short circuit between points P_1 and P_2, and degraded operation when only one path is healthy while the other one is faulty. The complete open circuit case or short circuit case between P_1 and P_2 result in unavailability of the normal services, while the third case results in degraded operation. The degraded operation case may lead to activation of the protection system if the fault current or the quality of the waveform is not satisfactory. In the following subsections the short circuit case and the loss of one of the drive signals (or fault in only one of the paths shown in Fig.5-b) as well as the behavior of proposed system under severe sensors fault are considered.

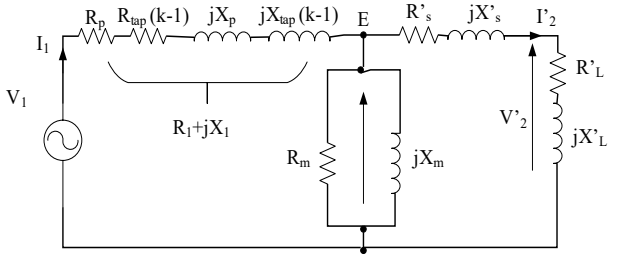

FIGURE 6. Tapped transformer operational equivalent circuit referred to the primary side.

1) INTER-TAP SHORT CIRCUIT ANALYSIS

Referring to Fig. 5-b, when short circuit occurs in both or one of the paths during the operation of switch number "*k*", the corresponding tap will continuously be connected. This continuous connection results in a short circuit operation between taps when the controller sends a command to transfer from one tap to another. Fig. 7 shows the tracing of the inter-tap short circuit current ($I_{tap\text{-}short}$) path during the simultaneous operation of switches S_k and S_{k+1}.

This article has been accepted for publication in a future issue of this journal, but has not been fully edited. Content may change prior to final publication. Citation information: DOI 10.1109/ACCESS.2021.3079507, IEEE Access

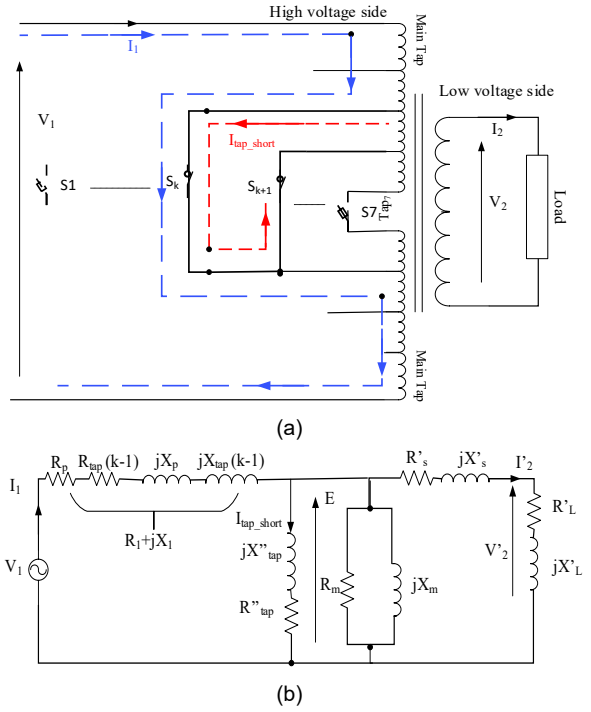

FIGURE 7. Current paths during inter-tap short circuit of S_K and S_{k+1}, (a) actual current paths (b) equivalent circuit refrred to primary side

The currents passing through switches S_k and S_{k+1} are (I_1 + I_{tap_short}) and I_{tap_short}, respectively. Equation (7) can approximate the current I_1, while the circulating short circuit current of I_{tap_short} can be calculated from the equivalent circuit shown in Fig.7. In this figure, the shorted tap works as a tertiary winding referred to the primary with turn's ratio from primary to the tertiary windings of:

$$a_{13} = \frac{N_{11} + (k-1)N_{tap}}{N_{tap}} \tag{9}$$

Using (10), the short circuit current I_{tap_short} can be calculated as:

$$I_{tap\_short} = \frac{E}{R''_{tap} + jX''_{tap}} = \frac{V_1}{(R''_{tap} + jX''_{tap})(R_1 + jX_1)} * \left(\frac{1}{\frac{1}{R_m} + \frac{1}{jX_m} + \frac{1}{R_1 + jX_1} + \frac{1}{R'_2 + jX'_2}} \right) \tag{10}$$

Alternatively, we can approximate the actual short circuit current passing through the switches as:

$$I_{tap\_short}(actual) = \frac{V_{tap}}{R_{tap} + jX_{tap}} = \frac{V_1 / a_{13}}{(R_{tap} + jX_{tap})} \tag{11}$$

Since the leakage inductance and resistance of the transformer tap windings are very small, the induced tap voltage results in large circulating current. The generated short circuit current will not appear in the input or output of the transformer terminals, but it will circulate between switches S_k and S_{k+1} and the connected tap windings. This short circuit can result in a permanent damage to the switches and the transformer winding insulation. Using fast-melting semiconductor fuses such as "Protistor" connected in series with the switches can provide protection to switches and transformer winding during such a short circuit. The short circuit current that can be calculated as given in (10) and (11) determines the rating of these fuses. In addition, the programming of control algorithm can achieve extra protection by ensuring that no two switches work simultaneously.

2) FAULT DUE TO LOSS OF DRIVE SIGNALS

During the loss of one of the drive signals G_1 or G_2, or generally when only one path between P_1 and P_2 (Fig.5-b) is healthy and the other one is faulty, only half-wave of the input voltage passes to the transformer primary winding.

Assuming one half cycle of the instantaneous sinusoidal voltage $v_1(t)=V_m \sin \omega t$, where ω is the fundamental angular frequency and V_m is the amplitude. The input voltage components in the transformer windings using Fourier series [29] can be expressed as:

$$v_1(t) = \frac{V_m}{\pi} + \frac{V_m}{2}\sin \omega t + \sum_{n=2,4,6,\ldots}^{\infty} \frac{V_m}{\pi} * \frac{1+(-1)^n}{1-n^2} \cos n\omega t \tag{12}$$

Equation (12) shows that the input voltage is composed of a considerable DC component (32% of V_m), fundamental component (50% of V_m), and a wide range of even harmonics whose amplitudes decrease quickly beyond the 4th harmonics.

Using superposition theorem and the equivalent circuit shown in Fig. 6, the DC input voltage component V_m/π results in a very large DC current given by:

$$I_{1\_DC} = \frac{V_m}{\pi} \frac{1}{R_p + (k-1)R_{tap}} \tag{13}$$

The only impedance opposing the flow of the DC current in (13) due to the DC component voltage is the leakage resistance of the primary winding. This current ($I_{1\text{-}DC}$) does not flow in the secondary winding, but it circulates between the supply and the transformer primary winding, which results in semi-short circuit condition. The fundamental component in (12) operates the transformer normally in a reduced

This article has been accepted for publication in a future issue of this journal, but has not been fully edited. Content may change prior to final publication. Citation information: DOI 10.1109/ACCESS.2021.3079507, IEEE Access

input voltage mode, and it results in scaled fundamental current components I_1 and I_2.

The even harmonic voltages in (12) emanate even current harmonics in the primary and the secondary circuit. Using (5)-(8), and (12) the values of these even harmonics' have been calculated as:

$$E_{-n} = \frac{V_{1-n}}{R_1 + jX_{1-n}} * \left(\frac{1}{\frac{1}{R_m} + \frac{1}{jX_{m-n}} + \frac{1}{R_1 + jX_{1-n}} + \frac{1}{R'_2 + jX'_{2-n}}} \right) \quad (14)$$

$$I_{1-n} = \frac{V_{1-n} - E_{-n}}{R_p + (k-1)R_{tap} + j(X_{p-n} + (k-1)X_{tap-n})} \quad (15)$$

$$I_{2-n} = \frac{E_{-n}}{R'_2 + jX'_{2-n}} * \left(\frac{N_{11} + (k-1)N_{tap}}{N_2}\right) \quad (16)$$

In (14)-(16), "n" stands for the even harmonic order, and all the inductance values must be recalculated corresponding to the harmonic order.

In the above equations (13)-(16), the DC current component in the primary side is high and may exceed the fundamental component. The even harmonic currents produced in the primary side lead to propagation of even current harmonics in the secondary side, which result in deformed secondary voltage and current. Keeping in mind that the transformer primary multitaps are electrically isolated from the secondary windings, which provides an acceptable level of galvanic isolation. Hence, the DC component cannot pass to the transformer's secondary side. The resultant primary current (DC component plus even harmonics plus fundamental) is extremely large than the normal operating current. This high non-sinusoidal current leads to degrading operation of the system and may result in system unavailability. One of the possible solutions of this type of faults is to use redundancy of switching system (Power electronics elements plus drive circuit), which means using parallel IGBTs module such as TIDA 00917. This solution increases the reliability of switching system. However, the cost will increase.

3) FAULTS DUE TO SENSORS FAILURE

Referring to the control block diagram in Fig. 2 and the control algorithm in (2), complete failures in the secondary voltage sensor ($V_{2\text{-}rms}$) or the secondary reference voltage (V_{ref}) result in relatively large "ΔV" calculation, which shifts the voltage error to be in the range (ΔV>7h or ΔV<-7h). In this situation, the control algorithm activates the centre tap (tap 4) as given in (2); and minimizes momentarily the power interruption to consumers under uncontrolled voltage operating mode for one period time. However, the loss of the input voltage sensor ($V_{primary}$) is critical since it gives indication of working beyond the input voltage range (extreme high input voltage or extreme low input voltage), in which case the control algorithm switches off the transformer and results in system unavailability.

Faults in the primary current sensor ($I_{primary}$) yields inaccurate detection of the zero crossing instants and this in turn results in possible high transient voltage at IGBT gate turn-off. This uncontrolled transient voltage can exceed the blocking voltage rating of the IGBT and cause it to fail [30]. To minimize the effect of this transient voltage in this work, the region of the zero detection is increased to be within certain minimum current range (I= ±10 mA), additionally snubber capacitors have been used as shown in Fig.1. It is worthy to mention that the snubber capacitor significantly reduces the voltage stress and switching losses during turn off [30].

C. COMPARISON WITH PREVIOUS DESIGN

To reflect its advantages, the proposed electronic onload tap changer system is compared with existing design as given in Table I. The selected designs for the comparison are: The design given in [18], (Thyristor based onload tap changer), the design presented in [20], (Bridge diode-IGBT based onload tap changer) and the design illustrated in [22], (IGBT based onload tap changer). The presented comparison considers the number and type of the power electronic elements (per one bidirectional switch), complexity of the drive and control circuit, voltage regulation capability, reliability, and amount of the power handling.

With reference to the comparison of Table I, the following points can be concluded:

- The thyristor based electronic tap changers have very slow switching speed and therefore they are unable to perform continuous voltage regulation and unable to correct sag and swell problems in distribution system. However, it can handle very high power at high voltages during tap switching.
- The IGBT based electronic tap changers are characterised by very high switching speed and can handle continuous voltage regulation.
- The reliability of the electronics onload tap changers depends on the combination of the power electronics elements to perform the required bidirectional switch. More elements in this switch result in poor reliability onload tap changer.

This article has been accepted for publication in a future issue of this journal, but has not been fully edited. Content may change prior to final publication. Citation information: DOI 10.1109/ACCESS.2021.3079507, IEEE Access

TABLE I: Comparisons of onload tap changers.

	Number & type of the switching elements	Drive and control circuit requirements	Continuous voltage regulation	Reliability and faults consideration	Power handling capability
Design of [18]	4 thyristors	Very complicated drive circuit and complicated control circuit (with overlap operation of the taps)	Uncapable to handle continuous voltage variation due to its slow switching rate	Unreliable as 4 controlled switches are required during one switching period	Very high
Design of [20]	4 diodes + 1 IGBT with anti-parallel diode	Simple drive circuit, however, the control circuit requires two step commutation for taps (short circuit overlap operation)	Its possible to perform fast voltage regulation and handle voltage flicker	Using of 6 elements per switching decreases the overall reliability. In addition, the construction of the multitaps windings in the secondary side provides no galvanic isolation.	Limited
Design of [22]	2 IGBT with antiparallel diodes	Simple drive circuit, with complex control circuit which requires transient short circuit overlap operation of the taps	It can perform fast voltage regulation and handle voltage variation	Though its relatively reliable in term of the switching units, the short circuit overlapping of the taps decreases its reliability	Limited
The proposed Design	2 IGBT with antiparallel diodes	Simple drive circuit and smooth control circuit without overlap operation of the taps	It is very effective in continuous voltage regulation.	Its relatively more reliable by adopting few microseconds dead time to replace the overlap operations of the tap in the above mentioned designs	Limited

- The proposed onload tap changer arrangement has moderate reliability, very fast switching rate, flexible control circuit and can compensate for transient voltage variation without short circuit overlap of taps switching.

IV. EXPERIMENTAL RESULTS AND DISCUSSION

A prototype of an electronic IGBT based on-load tap changer system has been experimentally built to test and verify the validity of the proposed system in section II, and to show its ability to regulate voltages in the distribution network. Fig.8 shows the experimental setup based on the proposed system. The transformer is a single-phase winding autotransformer equipped with 7 taps in the high voltage side, the parameters of the transformer are given in Table II.

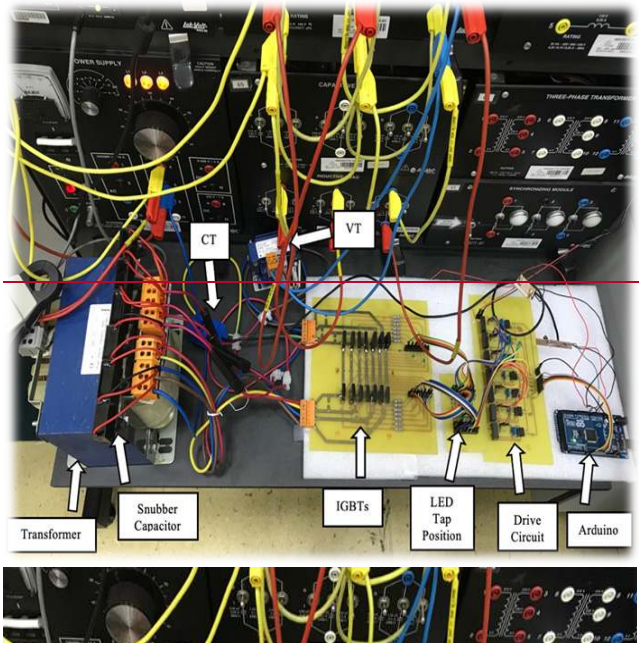

The control algorithm that follows the logic given in section II.A receives two input voltage values and the sensed input current. The voltages are instantaneously sensed using a designed and calibrated voltage transformer (VT). The control algorithm calculates the RMS value of the sensed instantaneous voltages during ½ cycle (10 ms). A current sensor of type SCT-30A measures the instantaneous input current. To detect the zero crossing instants, the control algorithm uses the output of the current sensor. Table III summarizes the values of the passive components and the model numbers of the sensors and different semiconductors utilized by the system.

The system outputs are measured in terms of voltages and currents with standard voltage probes (Pintek, DP-25) and standard current probes (OWAN, CP-05+). In addition, LabVolt software and its data acquisition system are used to extract the harmonics during faulty operation.

TABLE II: Parameters of the single-phase scaled-model 7-tap, 2.5 kVA, 50 Hz Dry type transformer

Parameter	VALUE
Input Voltage (Volt)	290-305-320-335-350-365-380 Volt
Output Voltage (Volt)	220 Volt
Input current (Amp)	6.6A (@ 380 Volt)
Output current (Amp)	11.4A
Main primary winding resistance and leakage inductance (R_p, Xp) Ω	(0.44, 0.26) Ω
Secondary winding resistance and leakage inductance (Rs, X_s) Ω	(0.334, 0.20) Ω
Resistance and leakage inductance of one tap windings; (R_{tap}, X_{tap}) Ω	(0.03, 0.0135) Ω
Core equivalent resistance and inductance in HVS, (R_m, X_m) kΩ	(3.94, 2.18) kΩ

This article has been accepted for publication in a future issue of this journal, but has not been fully edited. Content may change prior to final publication. Citation information: DOI 10.1109/ACCESS.2021.3079507, IEEE Access

TABLE. III
Model and specifications of the components used in the scaled-model IGBT on-load tap changer system

Description	Symbol	Model Number
Antiparallel connected IGBTs (with antiparallel diodes)	S1 to S14	FGH60N60SFD
Snubber Capacitor	Cs	2uF (CBB61)
Current Sensor	CT	SCT-013
Voltage Senser	VT	REC-1
Optocouplers in Drive circuit	Opt coupler	HCPL-3120
DC/DC converter (in drive circuit)	DC/DC	A_S-2WR2

A. VOLTAGE REGULATION

1) ZERO-CROSSING CURRENT

To minimize the voltage spike due to the commutation of the taps, the control algorithm carries out the switching at zero-crossing currents. In the proposed design system, the zero-detection code works well, while crossing from "+ve" to "-ve" or vice versa, the zero current is set at I < |10 mA|. Fig. 9 shows the switching at zero crossing currents compared to the case without zero crossing instant. Observe the high voltage spike at the switching instant when the zero-detection code is not used.

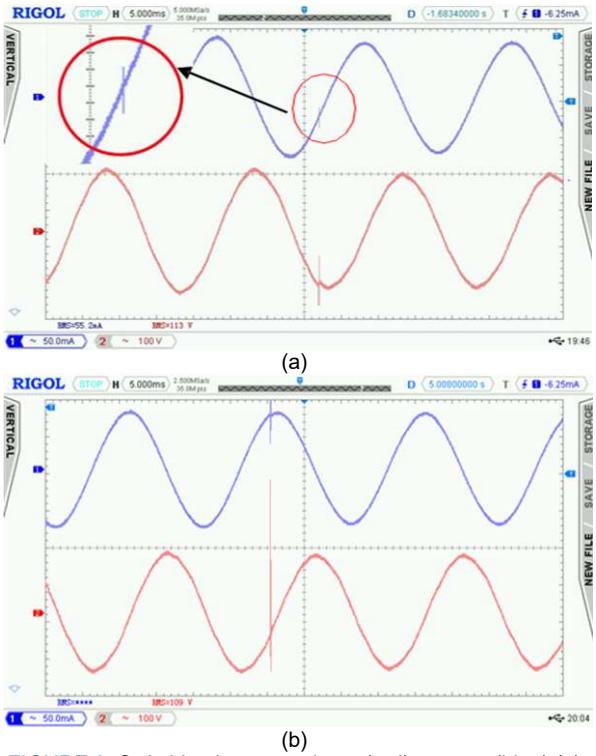

(a)

(b)

FIGURE 9. Switching instant, voltage (red), current (blue) (a) with zero crossing current (b) without zero crossing

2) STEADY STATE VOLTAGE REGULATION

The designed control algorithm has successfully achieved the steady state voltage regulation in the secondary side by automatic correction of the taps corresponding to the measured secondary and primary voltages. The selected regulation range of the load voltage is set as 100 ±5 Volt, the input RMS high voltage limitation is set as 180V and the low limitation is set as 60 volts. Fig.10 and Fig.11 depict samples of the automatic voltage and current regulation for some selected taps. Fig.10 shows the primary and secondary voltages during the activation of tap 1, tap 4, and tap 7. While Fig. 11 shows the corresponding primary and secondary current waveforms under the same loading condition.

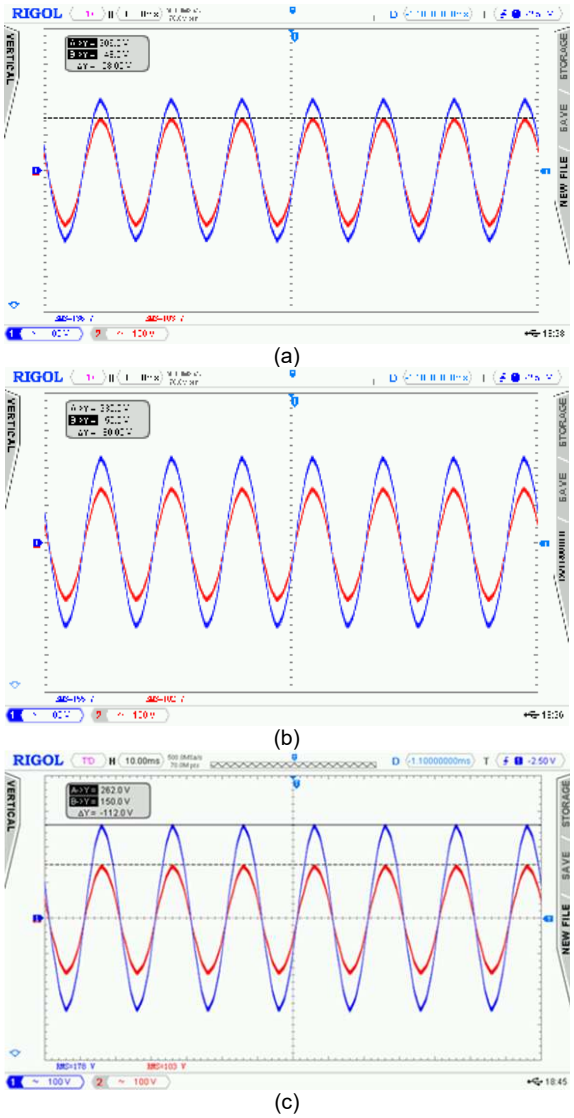

(a)

(b)

(c)

FIGURE 10. Primary (blue) and secondary (red) voltages during activation of (a) tap1, (b) tap4, and tap7.

We can observe from the above displayed figures that the proposed control algorithm and the designed system successfully have adjusted the secondary voltage into the allowable band variation of ±5V. All the secondary voltage values are in the range of 102-103 volt; irrespective of the input voltage whose recorded values are between 136V to 178V. Although the primary current has decreased from

This article has been accepted for publication in a future issue of this journal, but has not been fully edited. Content may change prior to final publication. Citation information: DOI 10.1109/ACCESS.2021.3079507, IEEE Access

42.5mA as shown in Fig. 11-a to 33.2mA as shown in Fig.11-c, the secondary current has remained almost at the value of 45.8 mA, which verifies the successful voltage regulation at the load side.

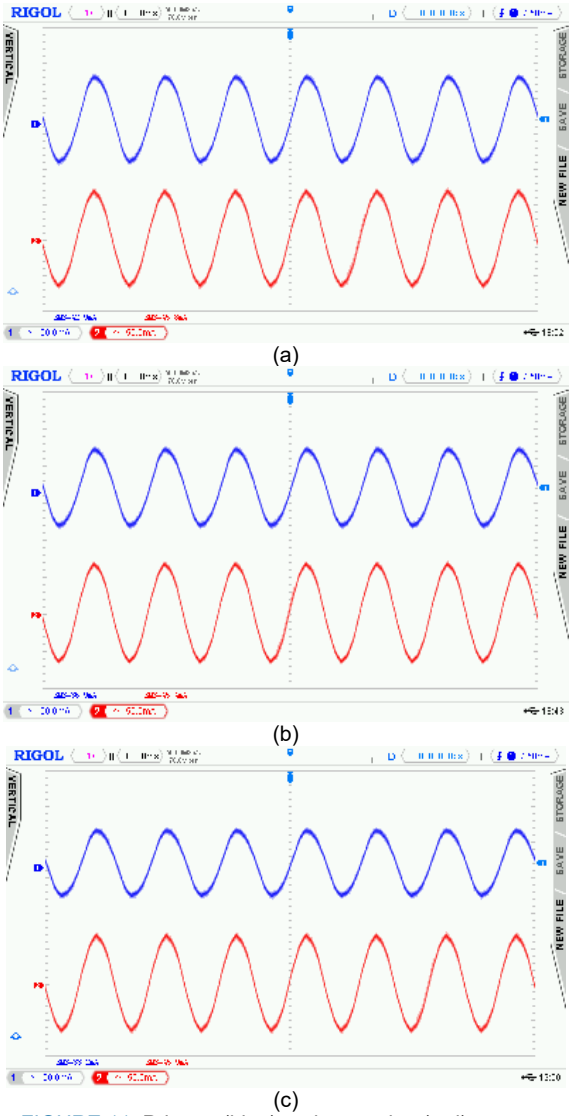

(a)

(b)

(c)

FIGURE 11. Primary (blue) and secondary(red) currents during activation of (a) tap1, (b) tap4, and tap7.

B. MITIGATION OF VOLTAGE SAG AND SWELL

To check the designed system stability response to a sudden voltage sag/swell in the primary side, the input voltage is adjusted to have sag of 74 volts (peak), where the input voltage is steadily decreased from 256 (peak) volt to 182 (peak) volt and increased back to its original value of 256 volt in 0.5 second. Fig. 12 depicts the system response in both the primary and the secondary voltage. Fig. 12 demonstrates that the designed system successfully absorbs the occurrence of the sag magnitude of 73.6 volt with a high response rate of not more than 1 cycle (20 ms), the system continuously and directly changes the taps corresponding to the measured voltage error and the current operating tap position within the allowable input voltage range. In Fig. 12, the regulated measured peak-peak voltage variation is 13.92 volt (9.2 vrms) in the secondary side, which is within the allowable range of the output voltage during the whole sag period.

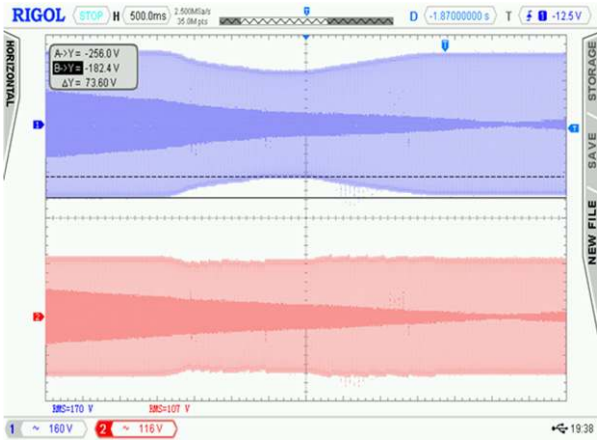

FIGURE 12. Primary input sag voltage variation (upper), and secondary output voltage response (lower)

Fig. 13 shows the response of the designed system to the tested voltage swell variation of magnitude 76.80 V (peak). The depicted secondary regulated voltage in Fig. 13 demonstrates that, the system positively responds to the input swell disturbance in the same manner as the case of the sag disturbance and produces regulated output voltage.

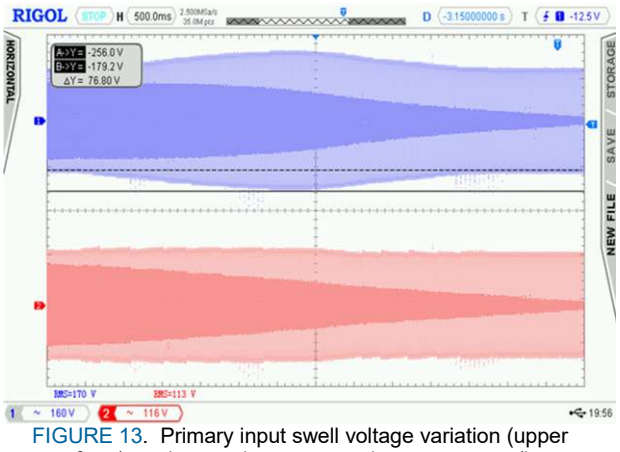

FIGURE 13. Primary input swell voltage variation (upper waveform), and secondary output voltage response (lower waveform)

C. FAULTS IN THE DRIVE CIRCUIT DUE TO LOSS OF GATE SIGNAL

The loss of the drive signal in one of the IGBTs in the bidirectional switch results in a deformation in the output voltage, and deformation in the input and output currents.

This article has been accepted for publication in a future issue of this journal, but has not been fully edited. Content may change prior to final publication. Citation information: DOI 10.1109/ACCESS.2021.3079507, IEEE Access

This type of fault (shown in section III.B.2) results in a large DC component in the input current. In addition, it may result in a false switching across the taps due to high dv/dt. Fig. 14 summarizes the behavior of the proposed system towards this type of fault. Fig.14-a shows the healthy system response of input voltage (Ch1), output voltage (Ch2), input current (Ch3) and output current (Ch4) compared to faulty system response in Fig. 14-b. The faulty system result is recorded during the loss of one IGBT drive signal of tap 4. The observed harmonics of the current in Fig. 14-d for the faulty system (as compared to the healthy one in Fig. 14-c) shows that the input current contains high DC current components that may exceed the fundamental component. In addition, it shows also considerable second harmonics (18% of the fundamental component) as well as some other harmonics. In result, the primary current shows a value of 0.71A (Fig. 14-b), which is more than 3 times of its value at normal operation (0.21A) as documented in Fig. 14-a. This result is matching the analysis given in section III.B.2. Hence, it can be concluded that loss of one drive circuit of the bidirectional switches may result in a very high fault current, which deteriorates the operation of the system, and eventually decreases its reliability.

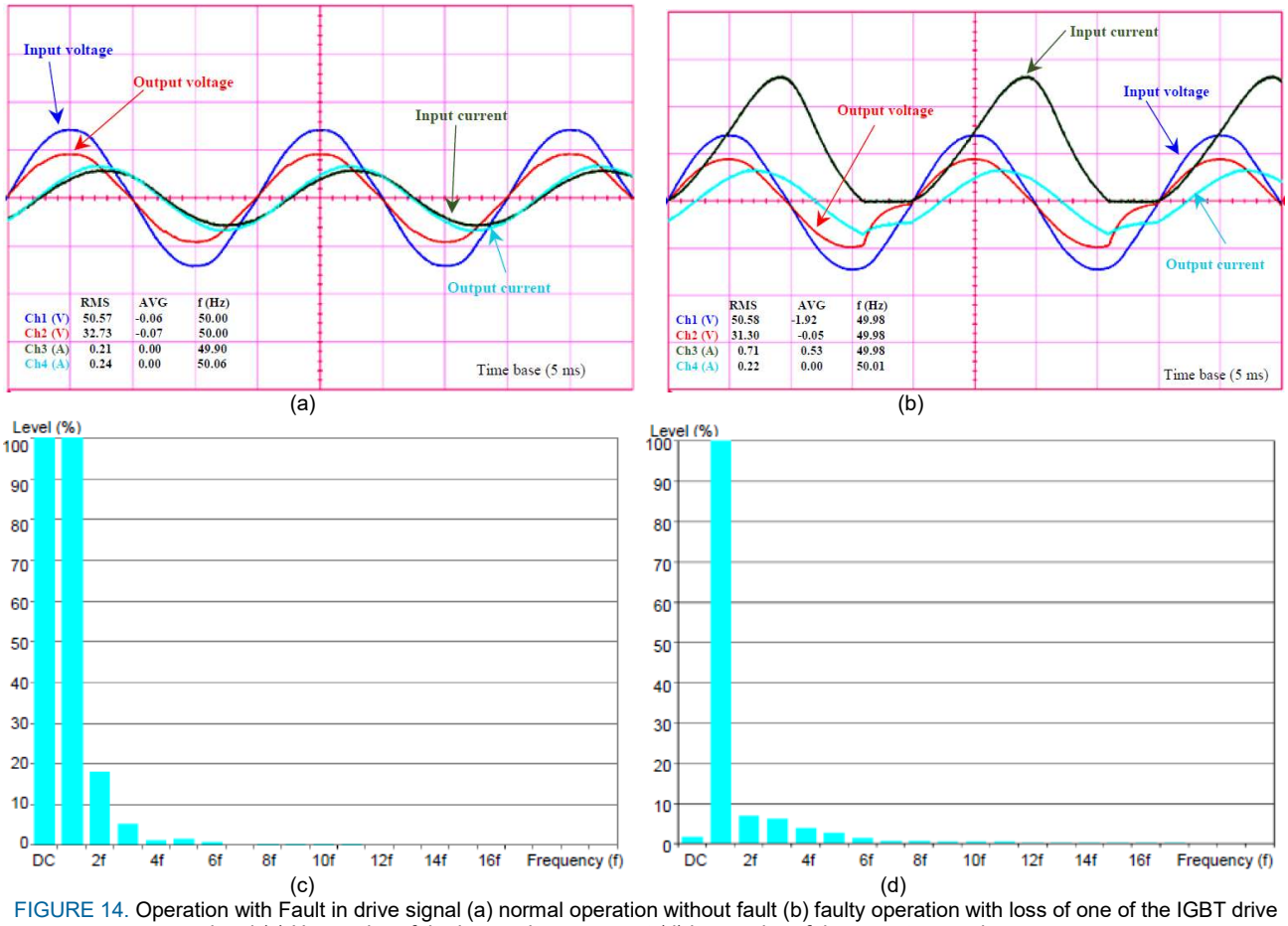

FIGURE 14. Operation with Fault in drive signal (a) normal operation without fault (b) faulty operation with loss of one of the IGBT drive signal (c) Harmonics of the input primary current (d) harmonics of the output secondary current.

V. CONCLUSION

The proposed OLTC system comprises a bidirectional IGBT arrangement connected in a common-emitter mode. The selected arrangement enables controlling the switching in one-step time, which reduces the level of the drive failure and increases its reliability. The proposed system comprises a unique nonlinear control system that, composes of a multilevel hysteresis controller and an inner limiter control loop. The designed control algorithm achieves a smooth and direct transition of the taps (without taps overlapping), which enables the designed OLTC to mitigate the sag and swell problems in a short response time.

The presented fault analysis shows that, the inter taps short circuit circulates a large current between the IGBT switches and the tap windings. This fault current results in a permanent damage to the switches and the transformer winding. Using fast-melting semiconductor fuses in series with the switches can provide an acceptable level of protection. The fault due to open circuit in one path of the bidirectional switching arrangement yields a very high DC

current and considerable harmonic components *in* the primary side. This high non-sinusoidal current (DC plus harmonics) yields degrading operation of the system and leads to system unavailability.

The propounded control algorithm provides partial protection to the system during transient fault of transformer secondary voltage sensor by activating the centre tap to minimize the power interruption to consumers. During the loss of the input voltage sensor the control algorithm switches off the transformer to prevent working under low or high input voltage.

The experimental results validate the performance of the proposed OLTC system for regulating the voltage and ensure the hazards of the fault analysis.

REFERENCES

[1] N. K. Roy and H. R. Pota, "Current status and issues of concern for the integration of distributed generation into electricity networks," IEEE System Journal, vol. 9, no. 3, pp. 933–944, Sep. 2015.

[2] R. Tonkoski, D. Turcotte, and T. H. M. EL-Fouly, "Impact of high PV penetration on voltage profiles in residential neighborhoods," IEEE Trans. Sustain. Energy, vol. 3, no. 3, pp. 518–527, Jul. 2012.

[3] T. Tewari, A. Mohapatra, and S. Anand, "Coordinated Control of OLTC and Energy Storage for Voltage Regulation in Distribution Network with High PV Penetration", IEEE Transaction on Sustainable Energy, Vol. 12, no. 1, pp 262-272, January 2021.

[4] N. Mahmud and A. Zahedi, "Review of control strategies for voltage regulation of the smart distribution network with high penetration of renewable distributed generation," Renewable Sustain. Energy Rev., vol. 64, pp. 582–595, 2016.

[5] T. Aziz and N. Ketjoy, ''Enhancing PV penetration in LV networks using reactive power control and on load tap changer with existing transformers,'' IEEE Access, vol. 6, pp. 2683–2691, 2018.

[6] C. R. Sarimuthu, V. K. Ramachandaramurthy, K. Agileswari, and H. Mokhlis, "A review on voltage control methods using on-load tap changer transformers for networks with renewable energy sources," Renew. Sust. Energy. Rev., vol. 62, pp. 1154–1161, 2016.

[7] M. Todorovski, "Transformer voltage regulation—Compact expression dependent on tap position and primary/secondary voltage," IEEE Transactions Power Delivery, vol. 29, no. 3, 1516–1517, 2014.

[8] H. Xu, A. D. Dominguez-Garcia, and P. W. Sauer, "Optimal Tap Setting of Voltage Regulation Transformers Using Batch Reinforcement Learning", IEEE Transaction on Power Systems, vol. 35, no. 3, pp. 1990-2001, May 2020.

[9] Georgios C. Kryonidis, Charis S. Demoulias, and Grigoris K. Papagiannis," A Two-Stage Solution to the Bi-Objective Optimal Voltage Regulation Problem," IEEE Transaction on Sustainable Energy, vol. 11, no. 2, pp. 928-937, April 2020.

[10] M. Bahadornejad and N. K. C. Nair, "Intelligent control of onload tap changing transformer," IEEE Transaction on Smart Grid, vol. 5, no. 5, pp. 2255– 2263, Sep. 2014.

[11] J. J. Erbrink et al., "Diagnosis of onload tap changer contact degradation by dynamic resistance measurements," IEEE Transaction on Power Delivery, vol. 25, no. 4, pp. 2121–2131, Oct. 2010.

[12] J. Faiz and B. Siahkolah, "Differences between conventional and electronic tap-changers and modifications of controller," IEEE Transaction on Power Delivery, vol. 21, no. 3, pp. 1342–1349, Jul. 2006.

[13] S. M. Garc´ia, J. C. C. Rodr´iguez, J. A. Jardini, J. V. Lopez, A. I. Segura, and P. M. M. Cid, "Feasibility of electronic tap-changing stabilizers for medium voltage lines—Precedents and new configurations," IEEE Transaction on Power Delivery, vol. 24, no. 3, pp. 1490–1503, Jul. 2009.

[14] G. R. C. Mouli and P. Bauer, "Design of a Power-Electronic-Assisted OLTC for Grid Voltage Regulation", IEEE Transaction on Power Delivery, Vol. 30, No. 3, pp. 1086–1095, June 2015.

[15] J. H. Shuttleworth, R. AlZahawi, and X. Tian, "A Fast Response GTO Assisted Novel Tap-Changer", IEEE Transactions on Power Delivery, Vol. 16, No. 1, pp.111-115, Jan. 2001.

[16] E. Martinez, I. Fernandez, and J. M. Canales, "Thyristor based solid state tap changer for distribution transformers," 2013 IEEE 11th International Workshop of Electronics, Control, Measurement, Signals and their application to Mechatronics, Toulouse, 2013, pp.1-5.

[17] E. Betancourt, O. Mendez, and D. Rivas, "Distribution transformer with electronic tap changer featuring robust low current zero switching," 2014 IEEE PES T&D Conference and Exposition, Chicago, IL, 2014, pp. 1-4.

[18] H. Ma, S. Gu, H. Wang, H. Xu, C. Wang, and H. Zhou, "On-load automatic voltage regulation system designed via thyristor for distribution transformer," 2017 20th International Conference on Electrical Machines and Systems (ICEMS), Sydney, NSW, 2017, pp. 1-5.

[19] N. M. Lokhande, S. Kulkarni, V. Ghone, V. Kikale and R. Patharkar, "Design and implementation of triac based on load tap changer with primary tapping's for constant output voltage," 2017 2nd International Conference for Convergence in Technology (I2CT), Mumbai, 2017, pp. 106-109.

[20] R. Echavarr´ia, A. Claudio, and M. Cotorogea, "Analysis, design, and implementation of a fast on-load tap changing regulator", IEEE Trans. Power Electronics, vol. 22, no. 2, pp. 527–534, Mar. 2007.

[21] J. O. Quevedo et al., "Smart distribution transformer applied to Smart Grids," 2013 Brazilian Power Electronics Conference, Gramado, 2013, pp. 1046-1053.

[22] J. de Oliveira Quevedo et al., "Analysis and Design of an Electronic On-Load Tap Changer Distribution Transformer for Automatic Voltage Regulation," IEEE Transactions on Industrial Electronics, vol. 64, no. 1, pp. 883-894, January 2017.

[23] B. Tabbache, A. Kheloui, M. E. H. Benbouzid, A. Mamoune and D. Diallo, "Research on Fault Analysis and Fault-Tolerant Control of EV/HEV Powertrain," IEEE ICGE 2014, Mar 2014, Sfax, Tunisia. pp. 284-289.

[24] B. Lu and S.K. Sharma, "A literature review of IGBT fault diagnostic and protection methods for power inverters," IEEE Transaction on Industry Applications, vol. 45, no 5, pp. 1770-1777, September/October 2009.

[25] M. E. H. Benbouzid, C. Delpha, Z. Khatir, S. Lefebvre and D. Diallo, "Faults Detection and Diagnosis in a Static Converter," Electrical Machines Diagnosis, Chap. 9, p. 271-316, ISBN: 978-1-84821-263-3, Wiley, ISTE, Paris 2011.

[26] R. R. Errabelli and P. Mutschler, "Fault-tolerant voltage source inverter for permanent magnet drives," IEEE Trans. Power Electronics, vol. 27, no 2, pp. 500-508, February 2012.

[27] C. C. Yeh and N.A.O., "Induction motor-drive systems with fault tolerant inverter-motor capabilities," in Proceedings of the 2007 IEEE, IEMDC, Antalya (Turkey), vol. 2, pp. 1451-1458, May 2007.

[28] J. Faiz and B. Siahkolah, "New solid-state onload tap-changers topology for distribution transformers," IEEE Trans. Power Del., vol. 18, no. 1, pp. 136–141, Jan. 2003.

[29] M. Rashid, "Power Electronics, Circuits, Devices and Applications", Pearson, ISBN: 0-13-101140-5, 3rd edition 2004, USA

[30] R. T. Naayagi, R. Shuttleworth and A. J. Forsyth, "Investigating the effect of snubber capacitor on high power IGBT turn-off," 2011 1st International Conference on Electrical Energy Systems, Chennai, India, 2011, pp. 50-55.
[30]

Ali A. Adam received his PhD degree in electrical engineering from Technical University of Yildiz, Istanbul, Turkey in 2007, M.Sc. degree from Bagdad University, Iraq, in 1997 and B.Sc. degree from University of Khartoum, Sudan, in 1991. His research interest includes control of electrical machines, power electronics applications, low frequency electromagnetic wave, filters, and smart grids.

Humaid Alsuwaidi graduated with BSc. Eng. degree in Electrical and Electronic Engineering from the University of Sharjah, United Arab Emirates in 2015**.** He is currently working in Dubai Electricity and Water Authority (DEWA)**.** His area of research interest focuses on distribution network, distribution transformer and voltage regulation using On Load Tap Changer (OLTC).

A. Elnady graduated from Cairo University, Cairo, Egypt, in 1990, where he received the Master degree in 1998. He got his Ph.D. degree in 2004 from the University of Waterloo, Waterloo, ON, Canada. His research interests include power-electronics applications in power systems, power quality in distribution systems, smart grids and integration of renewable sources within power grids.